



HAL
open science

Grain morphology memory : yttria as a study case

Jean-Marc Heintz, Agnès Dupont, Claude Parent, Bruno Le Garrec, Philippe Guionneau, Jean Etourneau

► **To cite this version:**

Jean-Marc Heintz, Agnès Dupont, Claude Parent, Bruno Le Garrec, Philippe Guionneau, et al.. Grain morphology memory : yttria as a study case. Key Engineering Materials, 2004, 264-268, pp.15-20. 10.4028/www.scientific.net/KEM.264-268.15 . hal-00159884

HAL Id: hal-00159884

<https://hal.science/hal-00159884>

Submitted on 5 Feb 2024

HAL is a multi-disciplinary open access archive for the deposit and dissemination of scientific research documents, whether they are published or not. The documents may come from teaching and research institutions in France or abroad, or from public or private research centers.

L'archive ouverte pluridisciplinaire **HAL**, est destinée au dépôt et à la diffusion de documents scientifiques de niveau recherche, publiés ou non, émanant des établissements d'enseignement et de recherche français ou étrangers, des laboratoires publics ou privés.

Grain Morphology Memory : Yttria as a Study Case

J. M. Heintz¹, A. Dupont^{1,2}, C. Parent¹, B. L. Garrec², P. Guionneau¹ and J. Etourneau¹

ICMCB-CNRS, Université Bordeaux 1, 87 Av. A. Schweitzer, 33608 Pessac Cedex (France)

² CEA/CESTA, 15 Av. des Sablières, BP n°2, 33114 Le Barp (France)

Keywords: chemical synthesis, grain shape, topochemistry, yttria

Abstract. This work shows how it is possible to orientate powder grain morphology characteristics through synthesis conditions **both** for **as-synthesized powders** ($T = 115^{\circ}\text{C}$) and for **calcined powders** ($T = 800$ or 1100°C). The chosen example deals with the synthesis of fine yttria powders, using chemical methods. As a first point of interest, the preparation of the as-synthesized powder is discussed. A sol-gel method has been developed in which the chemical nature of the yttrium chelating agent and the [chelating agent/Y] relative concentration are the two main parameters. Depending on these conditions, very different grain morphologies were obtained, needles, platelets, gel-like, in relation to the chemical and structural composition of these precursor powders. The second point of interest deals with the morphology of the yttria powder obtained after thermal treatment of these precursors at high temperature. In some cases, the original morphologies were maintained all over the calcining treatment whereas chemical composition changes were large. Thermodynamics consideration are also proposed to explain the final grain evolution at 1100°C . This yttria study case shows that a "memory effect" can actually be observed all over a large temperature range when the synthesis conditions constrain enough the precursor grain formation from a chemical and structural point of view.

Introduction

Controlling more and more precisely the size and the shape of the grains during synthesis is still today a real concern. In the case of oxide powders, many works have also been realized in order to propose various methods to adjust grain shape and grain size [3-12]. In the solvothermal process, solvent, pressure, temperature and precursor nature can be set to tailor grain shape and size. In others works related to sol-gel processes, the authors point out the effects of concentration, pH, aging time and synthesis temperature (from room temperature to 250°C aging temperature) on the final powder morphology [9-11]. Matrix mediated synthesis [12] can also be mentioned in which grain morphology depends on the polymer used as a matrix.

More precisely, concerning yttria synthesis, different routes have been studied. Thermal plasma processing allows a very good control of the size of the grain (around 20 nm) [13], whereas electrospray pyrolysis [14] leads to specific spheroidal shape and submicrometer size oxide particles (200 nm). Emulsion precipitation [15] also provides particles with spherical grain shape and submicronic particle size. Finally, hydroxide-gel precipitation method leads to submicronized but agglomerated yttria [16] while a sol-gel method is mentioned to give a friable oxide ash after calcination [17].

Now, only a few works can be mentioned concerning control of both size and shape of yttria powders in relation to the synthesis medium. In order to prepare spherical, monosized yttria particles, Sordelet and Akinc studied the effect of concentration and aging time [18] on particle morphology. It appeared that spherical grains can be obtained as long as the urea concentration was high enough while the shape of the grains can be influenced by the yttrium concentration and by the

nature of the counter anion relative to yttrium. Another work also suggested that the chelating media could have an influence on structural characteristics of obtained yttria particles [17].

Since the main objective of our work deals with the control of both size and shape of yttria particles in order to prepare a sinterable powder, we were interested in sol-gel like methods. Indeed, previous works related to oxides pointed out the role of chelating media on the microstructural characteristics of the fine powders in the case of urea [18] or polyacrylic acid [17]. Therefore, we extended this approach to the synthesis of yttria in such a manner to investigate the effect of the chelating agent and its relative concentration on particle morphologies and size, even after high temperature calcination treatment.

Experimental procedure

Yttria powders have been synthesized by a chemical route involving various organic acids : acetic ($C_2H_4O_2$), oxalic ($C_2H_4O_4$), malonic ($C_3H_4O_4$), tartaric ($C_4H_6O_6$) and citric ($C_6H_8O_7$). These compounds can act as chelating agents and present different characteristics such as carbon atom amount, carbonic chains length and “chelating claws”. Influence of their concentration on gel and powder characteristics has been studied : two different [chelating agent]/[Y] ratios (R) were considered, i.e. $R = 2$ and $R = 20$. pH was initially adjusted to $pH = 2$ in all cases. Organic acid was added to an yttrium nitrate solution until the chosen [chelating agent]/[Y] ratio was satisfied. The solution was then heated at $115^\circ C$ for 12 hours leading to the formation of a gel. Resulting products were then heat treated at $800^\circ C$ or $1100^\circ C$ for 4h. in a flowing oxygen atmosphere.

Results and Discussion

Gel characterization

XRD analysis of the materials obtained after heating at $115^\circ C$ (named as precursor gel) showed that they contained at least one crystallized phase, excepted for the citric acid route. In fact, it is known that the formation of amorphous material is favored when citric acid is used as a chelating agent [19]. The only pattern corresponding to a referenced phase was that of ammonium yttrium oxalate : $YNH_4(C_2O_4)_2 \cdot H_2O$ (JCPDS file n° 22-1047). All other crystallized phases were not known. It was checked that these phases did not correspond to starting compounds such as $Y(NO_3)_3$, or to salts coming from a basic combination of starting ions such as NH_4NO_3 . Now, three new phases have been identified and their structure has been resolved : for the malonate route with $R = 2$, it leads to $[Y(C_3H_2O_4)(H_2O)_4]NO_3$ ($R = 2$), with $R = 20$ to $[Y(C_3H_3O_4)_3(H_2O)_2] \cdot 3H_2O$ ($R = 20$) and for the acetate route with $R = 20$, it yields $[Y(CH_3CO_2)_3(H_2O)_2]$, $[Y(NO_3)_3(H_2O)_4] \cdot 2H_2O$ [20]. For other chelating agents, structures are still not determined but Infra-red and Raman complementary analyses have revealed low frequencies absorption bands that can be attributed to Y-O (belonging to the chelating agent) bonds [21].

As a conclusion, all experimental observations suggest that the gelification process leads, excepted for the citric acid route, to crystallized phases, including both yttrium and the corresponding organic acid. It means that the organic acid and its relative concentration should play a key role in the powder synthesis and the growth process.

Gel formation

As a matter of fact, conditions of formation of gels strongly depend on the nature of the organic acid. In the case of tartaric and oxalic acids, white precipitates immediately appeared while the solutions remained limpid for many hours in the case of other chelating agents and presented quite a higher viscosity.

Chelating agent geometry may be argued to account for these different behaviors. In the case of tartaric and oxalic acids, double chelating “claw” geometry may initiate quickly polymeric structure formation [22-23]. For other organic acids, only one chelating “claw” is acting (the other chelating functions that eventually exist only involve 4 atom-cycles and thus are not thermodynamically favored). Concerning gel viscosity, molecule geometry may, again, explain that behaviour differences. In the case of citric, malonic and acetic chelating agents, formation of the gel takes

place by solvent evaporation during heating which likely lead to the formation of hydrogen bonds after reducing the solution volume [24]. This was confirmed by infrared spectra analyses which exhibited a 500 cm^{-1} broad absorption band around $3500\text{-}3000\text{ cm}^{-1}$ (O-H stretching) corresponding to various length hydrogen bonds which bridge molecules and give a high viscosity to the gel precursor. On the other hand, in the case of oxalic and tartaric acids, only a sharp absorption band at 3500 cm^{-1} was observed which was related to O-H bonds belonging to crystallized phases (e.g. $\text{YNH}_4(\text{C}_2\text{O}_4)_2\cdot\text{H}_2\text{O}$) or to inter-chains or inter-planes bonds.

Precursor gel morphology

Precursor gel morphologies are illustrated in Fig. 1. No grain-like morphologies were observed for citric, malonic and acetic ($R = 2$) precursor gels. For the citric acid precursor gels (Fig. 1(e)), it corresponds quite well with its amorphous nature as revealed by XRD. For malonic (Fig. 1(b)) and acetic ($R = 2$) precursor gels, XRD and IR spectra (broad absorption band in the $3500\text{-}3000$ range) also suggested a low crystallinity of these materials. As a consequence, no defined grain shape is expected.

On the other hand, oxalic (Fig. 1(a)) and tartaric (Fig. 1(c) and (d)) routes leads to the formation of grains exhibiting very specific shapes such as platelets or needles depending on the chelating agent or the concentration ratio. Similar results have been found concerning rare earth oxalate and tartarate grain shape [25, 26]. Concerning the shape itself, a platelet or needle-like crystallite growth can be understood in relation to the oxalic acid specific conformation made of two opposite chelating functions in the same plane. Crystallite development is expected in chain or plane, alternating yttrium and chelating molecule while chains or planes are connected together by weaker bonds. Also, tartaric acid possesses many possibilities to chelate yttrium but only two of them involve a 6-atom cycle thermodynamically more stable than the other chelating cycles. These two chelation functions are in the same planar geometry than oxalic acid, which is therefore likely to induce plate or chain-like growth, so that macroscopic shape looks like platelets or needles. Differences in morphology observed between gel precursors with $R = 2$ and 20 ratios (tartaric acid Fig 1(c) and (d)) suggest that when acid concentration is in large excess, a complete 2D growth of particles is less favored than the needle shape growth. This observation appear in agreement with the easy formation of elongated grains during crystallization of pure tartaric acid.

These experiments tend to show that the morphology of the precursor gels can be largely influenced by the nature of the chelating agent. Moreover, it can be noticed that the concentration ratio also plays a role in that shape formation process.

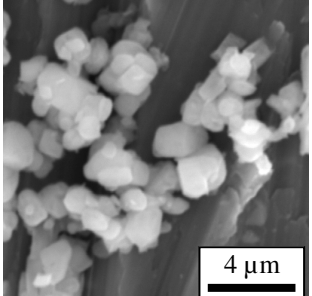
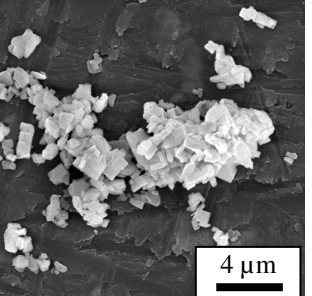
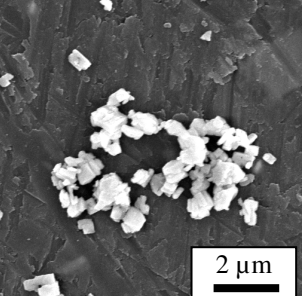
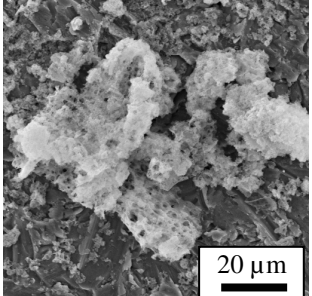
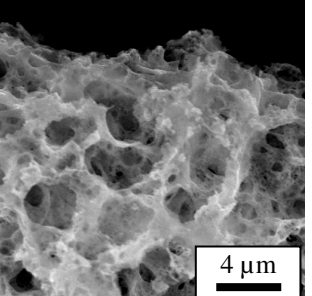
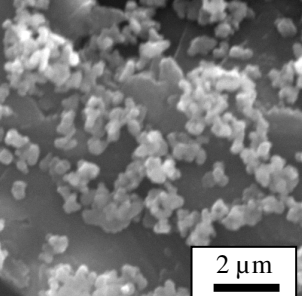
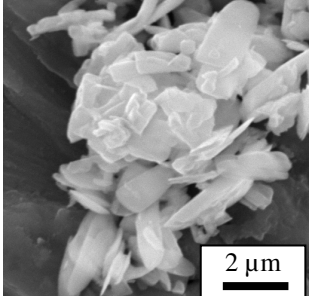
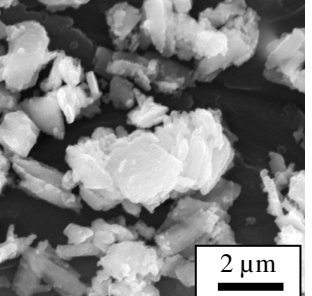
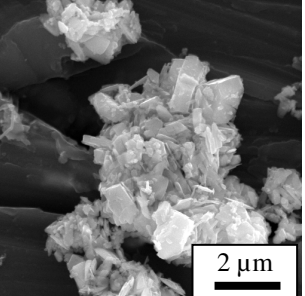
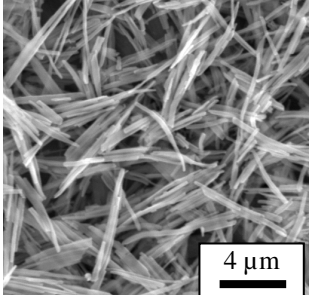
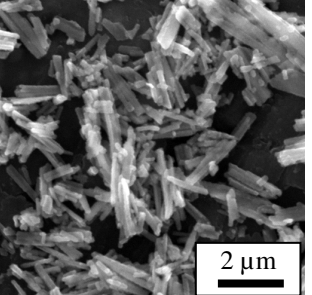
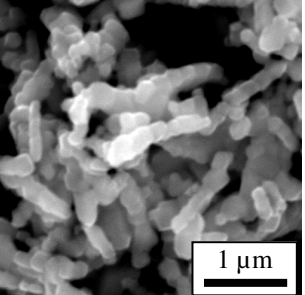
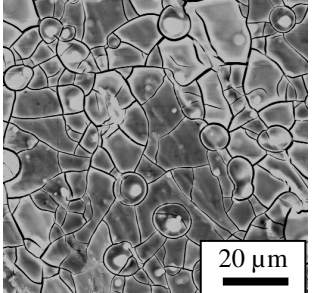
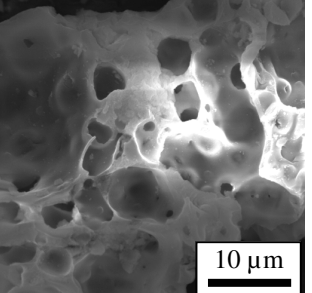
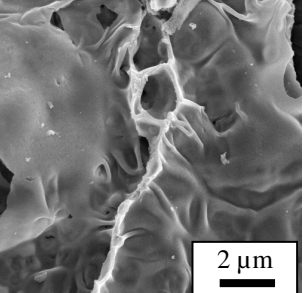
Precursor gel decomposition

Thermal treatment of precursor gels was always completed at 700°C . Of course, decomposition processes occurred in several steps that depended on the composition of the precursor gel. XRD analyses of the obtained powders showed that only cubic yttria was formed which lattice parameter corresponded to the theoretical one (JCPDS file n°86-1326).

Yttria powder morphology

Powder heat treated at 800°C

As it can be seen on SEM micrographs of yttria powders (Fig. 1, column 2), quite different morphologies were obtained. As in the case of precursor gels (column 1), the nature and the R ratio appear to play a key role on the shape of these grains. Moreover, a very strong relationship can be noticed between precursor gel and yttria grain respective morphologies. Needles, platelet-shapes or

Chelating acid and [acid]/Y ratio (R)	precursor gels before calcination	yttria powders after calcination at $T_{\text{calc}} = 800^{\circ}\text{C}$	yttria powders after calcination at $T_{\text{calc}} = 1100^{\circ}\text{C}$
(a) Oxalic (R = 2)			
(b) Malonic (R = 2)			
(c) Tartaric (R = 2)			
(d) Tartaric (R = 20)			
(e) Citric (R = 2)			

absence of definite shape for a given precursor gel actually lead to the same morphology for the corresponding yttria powder. Such a so-called “pseudomorphism” is a rare phenomenon since large chemical and structural rearrangements take place during calcination and transformation of the precursor gel into the yttria powder. It has only been observed on doped oxysulfide compounds [31] or on alumina obtained by a sol-gel process [32]. It means that powder structuring during gelification is important enough to be maintained even after calcinations especially when grain aspect ratio is large.

Powder heat treated at 1100°C

The results are presented in Fig. 1, column 3. Two different behaviors can be observed. For the first one, (oxalic, tartaric with $R = 2$ and citric acid routes) no drastic morphological changes occurs between 800°C and 1100°C. For the second one (tartaric with $R = 20$ and malonic acid routes), grains obtained at 800°C break up into finer grains when heated at 1100°C. For the tartaric acid route (Fig. 1(d)), needles divide into primary particles; for the malonic acid route (Fig. 1(b)), the foam collapses into nanometric spherical grains and for the acetic acid route, platelets break into smaller pieces. Such behaviors could seem inconsistent with usual grain growth phenomena occurring when temperature increases. In fact, morphological evolution of such grain systems can be predicted quite precisely considering a simple thermodynamic analysis [33-35]. The morphological evolution of a polycrystalline grain such as a needle or a thin platelet can be analyzed in term of surface energy : $E_{\text{surf}} = \gamma_s \cdot A_s + \gamma_b \cdot A_b$ where A_s is the grain surface area, A_b is the grain boundary area, γ_s is the surface energy and γ_b is the grain boundary energy. Then, depending on a grain aspect ratio parameter (thickness over length), the grain morphology evolves, according to the minimization of surface energy. Either a complete break up of the grain is observed for large aspect ratio, either only grain grooving is observed. In the case of malonic and acetic acid routes, a complete breaking phenomenon takes place for the powders calcined at 1100°C while for tartaric acid ($R = 20$), the grooving phenomenon is observed.

Conclusion

Through the study of yttria powder synthesis, the interest of controlled chemical route to obtained specific grain size and shapes has been shown. Moreover, it established a strong correlation between the morphological characteristics of the as obtained precursor gel and the final yttria powder corresponding to what is called a memory effect.

Acknowledgments

This work was sponsored by the Commissariat à l’Energie Atomique (CEA-CESTA) and the authors also wish to express their gratitude to Region Aquitaine for its financial support.

References:

- [1] S. Mathur, M. Veith, V. Sivakov, H. Shen and H-B. Gao, *J. Phys. IV*, 2001, **11**, 487-494
- [2] C.Y. Wang, G.M Zhu, S.L. Zhao, Z.Y. Chen and Z.G. Lin, *Mater. Res. Bull.*, 2001, **36** (13-14), 2333-2337
- [3] A.B. Velichenko, R. Amadelli, A. Benedetti, D.V. Girenko, S.V. Kovalyov and F.I. Danilov, *J. Electrochem. Soc.*, 2002, **149** (9), 445-449
- [4] T. Fukui, S. Ohara, M. Naito and K. Nogi, *J. Nan. Res.*, 2001, **3** (2-3), 171-174
- [5] Y.C. Kang, H.S. Roh and S.B. Park, *J. Electrochem. Soc.*, 2000, **147** (4), 1601-1603
- [6] Y.C. Kang, SB. Park, J.W. Lenggoro and K. Okuyama, *J. Electrochem. Soc.*, 1999, **146** (7), 2744-2747
- [7] T. Dubois and G. Demazeau, *Mater. Lett.*, 1994, **19** (1-2), 38-47
- [8] J.G. Darab and D.W. Matson, *J. Electron. Mater.*, 1998, **27** (10), 1068-1072
- [9] J. Livage, C. Sanchez, M. Henry and S. Doeuff, *Solid State Ionic*, 1989, **32-33** (2), 633-638

- [10] H. Fukui, H. Nishimura, H. Suzuki and S. Kaneko, *J. Ceram. Soc. Jpn.*, 1996, **104** (6), 540-544
- [11] E. Matijevic, *Ann. Rev. Mater. Sci.*, 1985, **15**, 483-516
- [12] S. Radhakrishnan and C. Saujanya, *Mater. Lett.*, 1996, **28** (4-6), 341-346
- [13] G.J. Vogt, *Proc. Electrochem. Soc.*, 1987, **87** (2), 1363
- [14] A.J. Rulison and R.C. Flagan, *J. Am. Ceram. Soc.*, 1994, **77** (12), 3244-3250
- [15] A. Celikkaya and M. Akinc, *Ceram. Trans.*, 1988, **1**, 110-118
- [16] P. Duran, P. Recio, J.R. Jurado, C. Pascual and C. Moure, *Ceram. Trans.*, 1988, **1**, 70-78
- [17] A.L. Micheli, *Ceram. Trans.*, 1988, **1**, 102-109
- [18] D. Sordélet and M. Akinc, *J. Colloid Interface Sci.*, 1988, **122**, 47-49
- [19] P.A. Lessing, *Ceram. Bull.*, 1989, **68** (5), 1002-1007.
- [20] P. Guionneau, A. Dupont, J.M. Heintz and C. Parent, to be published
- [21] A. Dupont C. Parent, J. Etourneau and J.M. Heintz, *Chem. Mat.*, submitted 2003
- [22] E. Hansson, *Acta. Chem. Scand.*, 1970, **24** (8), 2969-2982
- [23] W. Ollendorf, F. Weigel, *Inorg. Nucl. Chem. Letters* , 1969, **5**, 263-269
- [24] A. Durupthy, A. Casalot, A. Jaubert in *Chimie organique*, Ed. Hachette, Paris, 1996
- [25] T.R.R. Mac Donald and J.M. Spink, *Acta. Crystallogr.*, 1967, **23**, 944-951
- [26] P. Pascal, in *Nouveau traité de chimie minérale*, Ed. Masson, Paris, 1959, 1003-1024
- [27] L. Fraigi, D.G. Lamas and N.E. Walsøe de Reça, *Nanostruct. Mater.*, 1999, **11**, 311-318
- [28] Y-S. Han and H-G. Kim, *J. Power Sources*, 2000, **88**, 161-168
- [29] F. Li, K. Hu, J. Li, D. Zhang and G. Chen, *J. Nucl. Mater.*, 2002, **300**, 82-88
- [30] Z. Yue, L. Li, J. Zhou, H. Zhang and Z. Gui, *Mater. Sci. Eng., B*, 1999, **64**, 68-72
- [31] J.M. Luiz, E.B. Stucchi and N. Barelli, *Eur. J. Solid State Inorg. Chem*, 1996, **33**, 321-329
- [32] A.C. Pierre, in *Introduction aux procédés sol-gel*, Ed. Septima, Paris, 1992, 138
- [33] K.T. Miller and F.F. Lange, *Acta Metall.*, 1989, **37**, 1343-47.
- [34] K.T. Miller, F.F. Lange and D.B. Marshall, *J. Mater. Res.*, 1990, **5**, 151-160.
- [35] J.M. Heintz, J.C. Bihir and J.F. Silvain, *J. Eur. Ceram. Soc.*, 1999, **19** , 1759-1767.